

Structure and decay width of Θ^+ in a one-gluon exchange model

H. Matsumura^{1,*} and Y. Suzuki^{2,†}

¹*Graduate School of Science and Technology,
Niigata University, Niigata 950-2181, Japan*

²*Department of Physics, Niigata University, Niigata 950-2181, Japan*

Abstract

The mass and decay width of the $\Theta^+(1540)$ with isospin 0 are investigated in a constituent quark model comprising $uudd\bar{s}$ quarks. The resonance state for the Θ^+ is identified as a stable solution in correlated basis calculations. With the use of a one-gluon exchange quark-quark interaction, the mass is calculated to be larger than 2 GeV, increasing in order of the spin-parity, $\frac{1}{2}^-$, $\frac{3}{2}^-$ and $\frac{1}{2}^+(\frac{3}{2}^+)$, and only the $\frac{3}{2}^-$ state has a small width to the nK^{*+} decay. If the calculated mass is shifted to around 100 MeV above the $N+K$ threshold, the $\Theta^+(1540)$ is possibly $\frac{1}{2}^+(\frac{3}{2}^+)$ or $\frac{3}{2}^-$, though in the latter case it cannot decay to the nK^+ channel. In addition it is conjectured that other pentaquark state with different spin-parity exists below the $\Theta^+(1540)$. The structure of the Θ^+ is discussed through the densities and two-particle correlation functions of the quarks and through the wave function decomposition to a baryon-meson model and a diquark-pair model.

PACS numbers: 14.20.-c; 12.39.Jh; 21.45.+v

Keywords: pentaquark; quark model; decay width; hidden color

arXiv:nucl-th/0601011v1 5 Jan 2006

*Electronic address: hideki@nt.sc.niigata-u.ac.jp

†Electronic address: suzuki@nt.sc.niigata-u.ac.jp

I. INTRODUCTION

Quark model succeeds to classify the hundreds of baryons and mesons. A constituent quark model well reproduces the mass spectra of these hadrons using a colored interaction of one-gluon exchange (OGE) type together with a phenomenological confinement potential [1, 2]. There are of course those hadrons which do not fit the prediction of the constituent quark model, e.g., $N(1440)$ (Roper resonance) and $\Lambda(1405)$. Recently, motivated by a theoretical prediction for an exotic baryon [3], some experimental groups have searched for it and reported the observation of $\Theta^+(1540)$ which has baryon number +1, strangeness +1 and a decay width of less than 25 MeV [4, 5, 6]. Its minimal quark content is $uudd\bar{s}$, so it is often called a pentaquark baryon. A reason why the Θ^+ attracts much interest is that it is truly exotic, its mass is about 100 MeV above the $N+K$ threshold, and its decay width appears to be very small nevertheless. The spin and parity of the Θ^+ has not yet been known, nor even the existence of the $\Theta^+(1540)$ seems to be established experimentally [7, 8].

The recent controversial status of the $\Theta^+(1540)$ warrants a careful study of this system. From a theoretical side a calculation of the pentaquark mass and its decay width is useful and important. It was speculated that the Θ^+ is a bound state of two highly correlated ud pairs (diquark) and \bar{s} [9] or it is a coupled system of a color antisymmetric ud diquark with a $ud\bar{s}$ triquark [10]. In these models the spin and parity of the Θ^+ was assumed to be $J^P = \frac{1}{2}^+$ to account for its small decay width.

Some dynamical calculations of the mass of the Θ^+ for different J^P states have been performed in constituent quark models [11, 12, 13, 14]. The quark model usually predicts a smaller mass for the negative parity Θ^+ than for the positive parity Θ^+ . In fact the ground state of the Θ^+ is $\frac{1}{2}^-$, but it was argued that the mass difference between the $\frac{1}{2}^-$ and $\frac{1}{2}^+$ states may become small or even be reversed for a certain type of flavor-spin dependent interactions acting between the quarks [15]. See a review article [16] for some theoretical attempts and problems which are discussed from a broad perspective.

All the calculations performed so far in the constituent quark model were based on a variational principle which can be applied to a bound state problem. Without giving a link between such a bound state calculation and a decay width, it is hard to quantify the width of the Θ^+ . Though there are some attempts to predict the decay width of the Θ^+ in the constituent quark model [12, 17, 18], either the unbound nature of the Θ^+ is not taken into account or the assumption of its structure is too simple. Moreover, the correlated motion among the five quarks is usually truncated in the orbital, spin, isospin and color degrees of freedom or in some of them apart from a calculation [13]. For example, a treatment of hidden color components is not quite clear. Though the colors of the quarks are uniquely coupled to a color singlet state in a baryon and a meson, we have several possibilities to get a color singlet pentaquark. Therefore it is desirable to carefully examine the role of the hidden color states in a variational calculation. This problem is avoided in Ref. [11] by averaging a confinement potential.

We will instead show that it is possible to predict the mass of the pentaquark even though the hidden color components are included in a calculation. A very recent quark model calculation with a scattering boundary condition [14] is perhaps the only one that has undertaken a prediction of the width of the Θ^+ . It is claimed there that a sharp resonance with $\frac{1}{2}^-$ appears above 2 GeV, which is in disagreement with the other predictions [12, 18]. In any case, the appearance of such a narrow resonance is hard to understand unless the Θ^+ has negligibly small NK component. It is fair to say that the quark model study has not

so far given a settled prediction for the decay width of the Θ^+ though it seems to predict more or less a similar mass for it.

The purpose of this study is to predict the mass and the decay width of the Θ^+ in a few-body approach based on the quark model. We assume that the Θ^+ is a five-particle system but not a heptaquark system like $K\pi N$ [19], as discussed in [20]. We calculate the mass and the width for some J^P states assuming that the system has isospin 0 and is confined in a spatially small region. We pay a special attention to the unbound nature of the sought solution and perform a dynamical calculation which allows for not only spatial correlations among the quarks but also all possible spin-isospin-color configurations. The merit of employing the quark model is that it exploits the symmetry of the system and can test the validity of some models through the dynamical calculation. In this way, we can learn the extent to which the diquark model [9] or the diquark-triquark model [10] is sound. Also our model can include the effect of NK and NK^* channels on the Θ^+ , which is vital to predict the width.

We use a correlated Gaussian basis and a complete set of the spin-isospin-color configurations. To predict the mass and decay width of the Θ^+ , we use a real stabilization method [21] which utilizes square-integrable basis functions to localize the resonance. We use a stochastic variational method [22, 23] (SVM) to set up the basis set which describes resonance states. Our emphasis here is not to include continuum states explicitly but to localize the resonance in a simple way, which makes it possible to calculate the reduced width. We believe that to evaluate the decay width is still a worthwhile study, considering the present controversial situation as mentioned above.

The composition of the paper is as follows. Our formalism is explained in sect. II. We use an OGE potential as the interaction between the quarks, as defined in sect. II A. Some details are given for the basis function in a particular representation in sect. II B and for its transformation to other basis functions in sect. II C. The application of the real stabilization method to the description of a resonance is presented in sect. III. Here we illustrate an emergence of a unique solution (resonance) in the bound-state-looking calculations. The results of calculation are presented in sect. IV. The mass spectrum of the Θ^+ is given in sect. IV A, the decay width is discussed in sect. IV B, and the structure of the Θ^+ is analyzed in sect. IV C. A summary is given in sect. V.

II. FORMALISM

A. Hamiltonian

A Hamiltonian for the Θ^+ reads as

$$H = \sum_{i=1}^5 m_i + \sum_{i=1}^5 \frac{\mathbf{p}_i^2}{2m_i} - T_{\text{c.m.}} + \sum_{i<j} V_{ij}, \quad (1)$$

where m_i is the mass of the i th quark and V_{ij} is the interaction potential between the quarks. The so-called natural units are used, so a length has a dimension of inverse energy ($1 \text{ fm} = \frac{1}{197.3} \text{ MeV}^{-1}$). The kinetic energy of the quark is given in a nonrelativistic form and the kinetic energy of the center of mass motion, $T_{\text{c.m.}}$, is subtracted from the Hamiltonian. The eigenvalue of the Hamiltonian corresponds to the intrinsic mass of the Θ^+ .

The quark-quark potential used in this paper consists of a variant of OGE potential, a phenomenological confinement potential and a zero-point energy term. It is taken from

literatures: AL1 potential [2]

$$V_{ij} = -\frac{3}{8}(\lambda_i^C \cdot \lambda_j^C) \left(-\frac{\kappa}{r_{ij}} + \lambda r_{ij} - \Lambda + \frac{2\pi\kappa'}{3m_i m_j} \frac{\exp(-\frac{r_{ij}^2}{\rho_{ij}^2})}{\pi^{3/2}\rho_{ij}^3} \sigma_i \cdot \sigma_j \right), \quad (2)$$

with $\rho_{ij} = A \left(\frac{2m_i m_j}{m_i + m_j} \right)^{-B}$ or TS potential [11]

$$V_{ij} = (\lambda_i^C \cdot \lambda_j^C) \frac{\alpha_S}{4} \left\{ \frac{1}{r_{ij}} - \frac{e^{-\Lambda_g r_{ij}}}{r_{ij}} - \left(\frac{\pi}{2m_i^2} + \frac{\pi}{2m_j^2} + \frac{2\pi}{3m_i m_j} (\sigma_i \cdot \sigma_j) \right) \frac{\Lambda_g^2 e^{-\Lambda_g r_{ij}}}{4\pi r_{ij}} \right\} - (\lambda_i^C \cdot \lambda_j^C) a_{\text{conf}} r_{ij} + v_0. \quad (3)$$

Both potentials contain the color Coulomb and color magnetic terms.

λ_i^C are the color SU(3) generators (Gell-Mann matrices) for the i th quark. In this paper an SU(3) representation is labeled by Elliott's convention [24] $\Gamma = (\lambda\mu)$ whose dimension is $d(\lambda\mu) = \frac{1}{2}(\lambda+1)(\mu+1)(\lambda+\mu+2)$. A quark carries a color of (10) representation and an antiquark carries that of (01) representation. The color state of two quarks is either (20) (color symmetric) or (01) (color antisymmetric). Corresponding to these representations, the matrix of $(\lambda_i^C \cdot \lambda_j^C)$ becomes

$$(\lambda_i^C \cdot \lambda_j^C) = \begin{pmatrix} \frac{4}{3} & 0 \\ 0 & -\frac{8}{3} \end{pmatrix}. \quad (4)$$

For the case of a quark-antiquark pair the color state is either (11) or (00), and the matrix of $(\lambda_i^C \cdot \lambda_j^C)$ corresponding to these states is

$$(\lambda_i^C \cdot \lambda_j^C) = \begin{pmatrix} \frac{2}{3} & 0 \\ 0 & -\frac{16}{3} \end{pmatrix}. \quad (5)$$

In cases where the two quarks are in the color state (20) or the quark-antiquark pair is in (11), $(\lambda_i^C \cdot \lambda_j^C)$ gives a sign opposite to the physical cases which appear in a baryon and a meson, so those color states play a role of deconfining the quarks at large distances. We will not exclude such color states, however, from the beginning as they may be important in the Θ^+ comprising four quarks and one antiquark in a spatially confined region.

For a color singlet system, the zero-point energy term has an expectation value

$$\left\langle \sum_{i < j} (\lambda_i^C \cdot \lambda_j^C) \right\rangle_{(00)000} = \left\langle \frac{1}{2} \left(\sum_i \lambda_i^C \right)^2 - \frac{1}{2} \sum_i (\lambda_i^C)^2 \right\rangle_{(00)000} = -\frac{8}{3}n, \quad (6)$$

where the subgroup label of the color singlet state is denoted 000, and where n is the total number of quarks and antiquarks contained in the system and it determines the expectation value independently of the way of constructing the color state. Thus the zero-point energies of the AL1 potential are -2Λ , -3Λ and -5Λ , for mesons, baryons and the Θ^+ , respectively. In the case of the TS potential, v_0 is varied depending on n : $v_0 = V'_0$ for the meson, $v_0 = 3V'_0$ for the baryon, and $v_0 = 5V'_0$ for the Θ^+ . To change the parameter of the zero-point energy results in simply shifting the mass but never alters the eigenfunction of the Hamiltonian. This property will be used in sect. IV B to estimate the decay width of the Θ^+ .

We list in Table I the masses of some mesons and baryons calculated using the SVM [22, 23]. The parameters of the potential are also given in the table. It is found that both potentials give the results which agree reasonably well with the observed masses of $K, K^*, N(939)$ and $\Delta(1232)$. The $N + K$ threshold is 1486 and 1451 MeV for the AL1 and TS potentials, respectively. The masses of the strange baryons predicted with the TS potential are considerably large compared to the experiment, which is probably due to the fact that the mass of the strange quark is taken to be large. The masses of some baryons such as $N(1440)$ and $\Lambda(1405)$ are found to be too large. A flavor-dependent potential or some multi-quark configurations may be needed to reproduce these masses [25, 26]. The root mean square (rms) radius of the quark distribution is also calculated and listed in the table. The calculated size of $N(939)$ is apparently too small, so we must make allowance for this underestimation in setting a channel radius which is needed to calculate the decay width of the Θ^+ .

B. Basis function

Our Hamiltonian commutes with the total orbital angular momentum, the total spin and the total isospin. Thus the Θ^+ state is specified with their quantum numbers L, S and T . By letting J and P denote the total angular momentum and parity of the Θ^+ , we may write

TABLE I: The masses M and rms radii $\sqrt{\langle r^2 \rangle}$ of mesons and baryons. L is the total orbital angular momentum assumed in the calculation. The parameters for the AL1 potential [2] are $m_{ud} = 315$ MeV, $m_s = 577$ MeV, $\kappa = 0.5069$, $\lambda = 0.1653$ GeV², $\Lambda = 0.8321$ GeV, $\kappa' = 1.8609$, $B = 0.2204$, and $A = 1.6553$ GeV ^{$B-1$} , while those for the TS potential [11] are $m_{ud} = 313$ MeV, $m_s = 680$ MeV, $\alpha_S = 1.72$, $\Lambda_g = 3$ fm⁻¹, $\alpha_{\text{conf}} = 172.4$ MeVfm⁻¹, $V_0 = -345.5$ MeV, and $V'_0 = -742.7$ MeV.

Particle	L	AL1		TS	
		M [MeV]	$\sqrt{\langle r^2 \rangle}$ [fm]	M [MeV]	$\sqrt{\langle r^2 \rangle}$ [fm]
$\pi(138)$	0	138	0.30	106	0.32
$\rho(770)$	0	769	0.46	660	0.45
$K(496)$	0	491	0.31	514	0.33
$K^*(892)$	0	903	0.42	813	0.41
$N(939)$	0	995	0.49	937	0.50
$N(1440)$	0	1722	0.75	1755	0.73
$\Delta(1232)$	0	1307	0.58	1229	0.56
$\Lambda(1116)$	0	1148	0.47	1266	0.49
$\Lambda(1405)$	1	1522	0.58	1736	0.60
$\Sigma(1193)$	0	1229	0.49	1381	0.51
$\Xi(1318)$	0	1349	0.44	1659	0.49
$\Omega(1672)$	0	1675	0.48	2084	0.50

its wave function as an antisymmetrized product of the orbital, spin, isospin and color parts:

$$\Psi_{JM}^P = \mathcal{A} \left\{ [\psi_L^{(\text{orbital})} \psi_S^{(\text{spin})}]_{JM} \psi_{TM_T}^{(\text{isospin})} \psi_{(00)000}^{(\text{color})} \right\}, \quad (7)$$

where \mathcal{A} is an antisymmetrizer of the four quarks ($uudd$) labeled 1, 2, 3, and 4 (\bar{s} is labeled 5) normalized to $\mathcal{A}^2 = \mathcal{A}$, the square bracket $[\psi_L^{(\text{orbital})} \psi_S^{(\text{spin})}]_{JM}$ stands for the angular momentum coupling. The Θ^+ masses with different J values for a given set of L and S values are degenerate in our model.

Now we specify each part of Eq. (7) in detail. It is vital to allow for various types of correlation among the quarks. For the orbital part, we use an explicitly correlated Gaussian basis in a global representation [22, 23, 27]:

$$\begin{aligned} \psi_{LM_L}^{(\text{orbital})} &\sim \phi_{LM_L}(A, u, \mathbf{x}) = \exp \left\{ -\frac{1}{2} \tilde{\mathbf{x}} A \mathbf{x} \right\} \mathcal{Y}_{LM_L}(\tilde{u} \mathbf{x}) \\ &\equiv \exp \left\{ -\frac{1}{2} \sum_{i,j=1}^4 A_{ij} \mathbf{x}_i \cdot \mathbf{x}_j \right\} \mathcal{Y}_{LM_L} \left(\sum_{i=1}^4 u_i \mathbf{x}_i \right). \end{aligned} \quad (8)$$

where $\mathbf{x} = (\mathbf{x}_1, \mathbf{x}_2, \mathbf{x}_3, \mathbf{x}_4)$ stands for a set of the intrinsic Jacobi coordinates other than the center of mass coordinate of the system and it is defined from the single-particle coordinates of the quarks, $(\mathbf{r}_1, \mathbf{r}_2, \dots, \mathbf{r}_5)$, as usual. The angular motion of the system is described with a solid spherical harmonics $\mathcal{Y}_{\ell m}(\mathbf{r}) = r^\ell Y_{\ell m}(\hat{\mathbf{r}})$. Here a positive-definite, symmetric matrix A and a vector u are parameters which define the shape of the orbital part of the basis wave function. Note that u serves to define an appropriate coordinate responsible for the rotational motion of the system and that the spherical part of the orbital function can equivalently be expressed in terms of the relative distance vectors of the quarks:

$$\exp \left\{ -\frac{1}{2} \tilde{\mathbf{x}} A \mathbf{x} \right\} = \exp \left\{ -\sum_{l>k=1}^5 \alpha_{kl} (\mathbf{r}_k - \mathbf{r}_l)^2 \right\} \quad (9)$$

with appropriate α_{kl} 's. We use the correlated Gaussian because there are many examples which demonstrate its power for an accurate description of few-particle systems [22, 23]. Clearly our orbital part is translation-invariant, so our theory is free from any spurious center of mass motion. Note that the parity of the Θ^+ is given by $P = (-1)^{L+1}$ in the present formalism.

One of the most natural coupling schemes for the spin, isospin and color parts is to follow a successive coupling. The spin part may be expressed as

$$\psi_{SM_S}^{(\text{spin})} \sim \chi_{(S_{12}S_{123}S_{1234})SM_S}^{\text{SC}} = \left[\left[\left[[\chi_{\frac{1}{2}}(1) \chi_{\frac{1}{2}}(2)]_{S_{12}} \chi_{\frac{1}{2}}(3) \right]_{S_{123}} \chi_{\frac{1}{2}}(4) \right]_{S_{1234}} \chi_{\frac{1}{2}}(5) \right]_{SM_S}, \quad (10)$$

where $\chi_{\frac{1}{2}m_s}(i)$ is the spin function of the i th quark. Table II lists possible sets of $(S_{12}, S_{123}, S_{1234})$ for $S = \frac{1}{2}$ and $\frac{3}{2}$. For the isospin part we assume $T = 0$, $M_T = 0$. Because the \bar{s} does not carry an isospin, the isospin part can be given by coupling four $\frac{1}{2}$ angular momenta:

$$\psi_{TM_T}^{(\text{isospin})} \sim \xi_{(T_{12}T_{123}0)T=0M_T=0}^{\text{SC}} = \left[\left[\left[[\xi_{\frac{1}{2}}(1) \xi_{\frac{1}{2}}(2)]_{T_{12}} \xi_{\frac{1}{2}}(3) \right]_{T_{123}} \xi_{\frac{1}{2}}(4) \right]_{00} \xi(5), \quad (11)$$

TABLE II: Intermediate spin labels in different models

$S = \frac{1}{2}$									
Successive coupling			Diquark-diquark type			Baryon-Meson type			
S_{12}	S_{123}	S_{1234}	S_{12}	S_{34}	S_{1234}	S_{12}	S_{123}	S_{45}	
0	$\frac{1}{2}$	0	0	0	0	0	$\frac{1}{2}$	0	
0	$\frac{1}{2}$	1	0	1	1	0	$\frac{1}{2}$	1	
1	$\frac{1}{2}$	0	1	1	0	1	$\frac{1}{2}$	0	
1	$\frac{1}{2}$	1	1	0	1	1	$\frac{1}{2}$	1	
1	$\frac{3}{2}$	1	1	1	1	1	$\frac{3}{2}$	1	
$S = \frac{3}{2}$									
Successive coupling			Diquark-diquark type			Baryon-Meson type			
S_{12}	S_{123}	S_{1234}	S_{12}	S_{34}	S_{1234}	S_{12}	S_{123}	S_{45}	
1	$\frac{3}{2}$	2	1	1	2	1	$\frac{3}{2}$	0	
1	$\frac{3}{2}$	1	1	0	1	1	$\frac{3}{2}$	1	
0	$\frac{1}{2}$	1	0	1	1	0	$\frac{1}{2}$	1	
1	$\frac{1}{2}$	1	1	1	1	1	$\frac{1}{2}$	1	

where $\xi_{\frac{1}{2}m_i}(i)$ is the isospin function of the i th quark and $\xi(5)$ the ‘‘isospin’’ function of the $\bar{5}$. Possible values of (T_{12}, T_{123}) that enable one to make $T=0$, $M_T=0$ are $(0, \frac{1}{2})$ and $(1, \frac{1}{2})$. Similarly, the color part can be given, in the successive coupling, as

$$\begin{aligned} \psi_{(00)000}^{(\text{color})} &\sim C_{(\Gamma_{12}\Gamma_{123}\Gamma_{1234})(00)000}^{\text{SC}} \\ &= \left[\left[\left[C_{(10)}(1)C_{(10)}(2) \right]_{\Gamma_{12}} C_{(10)}(3) \right]_{\Gamma_{123}} C_{(10)}(4) \right]_{\Gamma_{1234}} C_{(01)}(5) \Bigg]_{(00)000}, \end{aligned} \quad (12)$$

where $C(i)$ stands for the color function of the i th quark, and the square bracket $[C_{\Gamma_1}C_{\Gamma_2}]_{\Gamma}$ denotes the SU(3) coupling of two functions with SU(3) irreducible representations Γ_1 and Γ_2 to that of a definite SU(3) representation Γ . Here Γ_{1234} must be (10) to make a color singlet Θ^+ . Possible sets of $(\Gamma_{12}, \Gamma_{123}, \Gamma_{1234} = (10))$ are listed in Table III. As seen from the table, three channels make a complete set for the color space of the Θ^+ .

To sum up, we may express a trial wave function for the Θ^+ as

$$\Psi_{JM}^P = \sum_{i=1}^{\kappa} C_i \Phi_i, \quad (13)$$

with the basis function

$$\Phi_i = \mathcal{A} \left\{ [\phi_L(A, u, \mathbf{x}) \chi_{(S_{12}S_{123}S_{1234})S}]_{JM} \xi_{(T_{12}T_{123})00} C_{(\Gamma_{12}\Gamma_{123}\Gamma_{1234})(00)000} \right\}, \quad (14)$$

where i stands for a set of $(A, u, S_{12}, S_{123}, S_{1234}, T_{12}, \Gamma_{12}, \Gamma_{123})$. Here T_{123} and Γ_{1234} are omitted as they have to be $\frac{1}{2}$ and (10), respectively. Note that the 4×4 matrix A is specified by ten parameters $(A_{11}, A_{12}, \dots, A_{44})$ or equivalently $(\alpha_{12}, \alpha_{13}, \dots, \alpha_{45})$ and the u by three

TABLE III: Intermediate color SU(3) labels in different models

Successive coupling			Diquark-diquark type			Baryon-Meson type		
Γ_{12}	Γ_{123}	Γ_{1234}	Γ_{12}	Γ_{34}	Γ_{1234}	Γ_{12}	Γ_{123}	Γ_{45}
(01)	(00)	(10)	(01)	(01)	(10)	(01)	(00)	(00)
(01)	(11)	(10)	(01)	(20)	(10)	(01)	(11)	(11)
(20)	(11)	(10)	(20)	(01)	(10)	(20)	(11)	(11)

parameters (as it can be set to a unit vector, $\tilde{u}u = 1$, without loss of generality). Thus we have 13 (10) continuous parameters for the basis function with $L \neq 0$ ($L = 0$) and in addition the spin-isospin-color channel label which is one of $5 \times 2 \times 3 = 30$ channels for $S = \frac{1}{2}$ or $4 \times 2 \times 3 = 24$ channels for $S = \frac{3}{2}$. We stress that all the possibilities satisfying the prescribed quantum numbers ($S, T = 0, \Gamma = (00)$) can be taken into account in the present formalism. Once the basis functions Φ_i are set up, the coefficients C_i and the eigenvalue M of the Hamiltonian can be determined by solving the following eigenvalue problem:

$$\sum_{j=1}^{\kappa} [\langle \Phi_i | H | \Phi_j \rangle - M \langle \Phi_i | \Phi_j \rangle] C_j = 0. \quad (15)$$

The label SC is omitted from the spin-isospin-color parts in Eq. (14) because other coupling schemes may be used equally well as explained below.

C. Transformation of basis

The successive coupling scheme introduced in sect. II B is systematic in its construction. The basis functions in that scheme constitute a complete set for specified quantum numbers and make it possible to represent any coupling schemes of physical interest.

The Θ^+ is considered a system of two diquarks and the \bar{s} in the diquark model [9], so it is useful to define the following coupling scheme, e.g., for the spin part

$$\chi_{(S_{12}S_{34}S_{1234})SM_S}^{\text{DD}} = \left[\left[\left[\chi_{\frac{1}{2}}(1) \chi_{\frac{1}{2}}(2) \right]_{S_{12}} \left[\chi_{\frac{1}{2}}(3) \chi_{\frac{1}{2}}(4) \right]_{S_{34}} \right]_{S_{1234}} \chi_{\frac{1}{2}}(5) \right]_{SM_S}. \quad (16)$$

Here one diquark has spin S_{12} and the other diquark S_{34} , and they are coupled to S_{1234} . We list possible sets of $(S_{12}, S_{34}, S_{1234})$ in Table II. As mentioned, this spin function can be expressed in terms of combinations of the spin functions in the successive coupling. This expansion can be represented as follows (by replacing the spin label S with J):

$$\text{Diagram 1} = \sum_{J_{123}} U(J_{12}J_3J_{1234}J_4; J_{123}J_{34}) \text{Diagram 2} \quad (17)$$

Here a Racah coefficient in unitary form, U , is expressed in terms of the $6j$ symbol

$$\begin{aligned} U(J_1 J_2 J J_3; J_{12} J_{23}) &= \langle (J_1 J_2) J_{12}, J_3; JM | J_1, (J_2 J_3) J_{23}; JM \rangle \\ &= (-1)^{J_1+J_2+J+J_3} \sqrt{(2J_{12}+1)(2J_{23}+1)} \left\{ \begin{matrix} J_1 & J_2 & J_{12} \\ J_3 & J & J_{23} \end{matrix} \right\}. \end{aligned} \quad (18)$$

To be more explicit, the spin function in the diquark model is transformed to the one in the successive coupling scheme by the matrix

$$\begin{pmatrix} 1 & 0 & 0 & 0 & 0 \\ 0 & 1 & 0 & 0 & 0 \\ 0 & 0 & 1 & 0 & 0 \\ 0 & 0 & 0 & -\sqrt{\frac{1}{3}} & \sqrt{\frac{2}{3}} \\ 0 & 0 & 0 & \sqrt{\frac{2}{3}} & \sqrt{\frac{1}{3}} \end{pmatrix} \quad \text{for } S = \frac{1}{2}, \quad (19)$$

and

$$\begin{pmatrix} 1 & 0 & 0 & 0 \\ 0 & \sqrt{\frac{2}{3}} & 0 & -\sqrt{\frac{1}{3}} \\ 0 & 0 & 1 & 0 \\ 0 & \sqrt{\frac{1}{3}} & 0 & \sqrt{\frac{2}{3}} \end{pmatrix} \quad \text{for } S = \frac{3}{2}. \quad (20)$$

Here the spin functions in both models are arranged in order of those defined in Table II.

Similarly, the color function in the diquark model can be expressed in terms of the successive coupling scheme. Possible sets of $(\Gamma_{12}, \Gamma_{34}, \Gamma_{1234})$ in the diquark model are listed in Table III. The transformation between the diquark coupling and the successive coupling can be performed using the formula (17) (by replacing the Racah coefficient with the corresponding one in the SU(3) algebra [28, 29]). Here the angular momentum label J should be understood to denote the color SU(3) label Γ . Note that all the SU(3) couplings appearing here are multiplicity-free. The color function in the diquark model is expressed in terms of the one in the successive coupling through the matrix

$$\begin{pmatrix} -\sqrt{\frac{1}{3}} & \sqrt{\frac{2}{3}} & 0 \\ \sqrt{\frac{2}{3}} & \sqrt{\frac{1}{3}} & 0 \\ 0 & 0 & 1 \end{pmatrix}. \quad (21)$$

A baryon-meson ($q^3-q\bar{q}$) coupling scheme is also important. Here three among the four quarks are coupled to a state with a definite spin, isospin and color, and the remaining quark and the \bar{s} are coupled to a state with given quantum numbers, and finally they are coupled to a resultant state. Again we can show this coupling scheme in a pictorial way and express it in terms of the successive coupling:

$$\begin{array}{c} \begin{array}{c} J_3 \\ \diagup \quad \diagdown \\ J_2 \quad J_4 \\ \diagdown \quad \diagup \\ J_1 \quad J_5 \\ \diagup \quad \diagdown \\ J_{12} \quad J_{45} \\ \diagdown \quad \diagup \\ J_{123} \quad J_{45} \\ \diagup \quad \diagdown \\ JM \end{array} \\ = \sum_{J_{1234}} U(J_{123} J_4 J J_5; J_{1234} J_{45}) \\ \begin{array}{c} \begin{array}{c} J_3 \\ \diagup \quad \diagdown \\ J_2 \quad J_4 \\ \diagdown \quad \diagup \\ J_1 \quad J_5 \\ \diagup \quad \diagdown \\ J_{12} \quad J_{123} \\ \diagdown \quad \diagup \\ J_{1234} \quad J_{45} \\ \diagup \quad \diagdown \\ JM \end{array} \end{array} \end{array} \quad (22)$$

Possible sets of $(J_{12}, J_{123}, J_{45})$ values in the baryon-meson coupling are listed in Table II for the spin part (χ^{BM}) and in Table III for the color part (C^{BM}), respectively. Note that Γ_{123} and Γ_{45} are not necessarily (00), that is, a colored baryon and a colored meson must be included to obtain a complete basis for a color singlet pentaquark. The spin function in the baryon-meson model is transformed to the one in the successive coupling by

$$\begin{pmatrix} -\frac{1}{2} & \frac{\sqrt{3}}{2} & 0 & 0 & 0 \\ \frac{\sqrt{3}}{2} & \frac{1}{2} & 0 & 0 & 0 \\ 0 & 0 & -\frac{1}{2} & \frac{\sqrt{3}}{2} & 0 \\ 0 & 0 & \frac{\sqrt{3}}{2} & \frac{1}{2} & 0 \\ 0 & 0 & 0 & 0 & 1 \end{pmatrix} \quad \text{for } S = \frac{1}{2}, \quad (23)$$

and

$$\begin{pmatrix} \sqrt{\frac{5}{8}} & -\sqrt{\frac{3}{8}} & 0 & 0 \\ \sqrt{\frac{3}{8}} & \sqrt{\frac{5}{8}} & 0 & 0 \\ 0 & 0 & 1 & 0 \\ 0 & 0 & 0 & 1 \end{pmatrix} \quad \text{for } S = \frac{3}{2}. \quad (24)$$

The color function in the baryon-meson model is transformed to that of the successive coupling by a unit matrix.

The Karliner-Lipkin model proposed in [10] considers the Θ^+ as a coupled system of a ud diquark and a $ud\bar{s}$ triquark. Here the ud pair in the diquark has $S_{12}=0$, $T_{12}=0$, $\Gamma_{12}=(01)$, and the other pair in the triquark has $S_{34}=1$, $T_{34}=0$, $\Gamma_{34}=(20)$. The quantum numbers of the triquark is $S_{345}=\frac{1}{2}$, $T_{345}=0$, $\Gamma_{345}=(10)$. Recoupling this configuration to the diquark-diquark model, we find that the Karliner-Lipkin model is reduced to one particular basis in the diquark model with $S_{1234}=1$, $T_{1234}=0$, $\Gamma_{1234}=(10)$, namely

$$\begin{array}{c} \text{00(01)} \\ \text{10(20)} \\ \text{1/2 0(10)} \\ \text{1/2 0(00)} \end{array} \text{1/2 0(01)} = \begin{array}{c} \text{00(01)} \\ \text{10(20)} \\ \text{10(10)} \\ \text{1/2 0(00)} \end{array} \text{1/2 0(01)} \quad (25)$$

The calculation of the decay width of the Θ^+ will be reduced to an overlap of the Θ^+ wave function with an nK^+ channel wave function. See sect. IV B. Here we write the spin-isospin-color part of the nK^+ channel wave function in terms of the successive coupling scheme. Both n and K^+ have isospin $\frac{1}{2}$ and only the isospin-singlet component of the coupled state contributes to the overlap with the Θ^+ wave function. The nucleon (N) is symmetric in its orbital space as well as in the spin-isospin space. Combining the transformation matrices given above, we can express the spin-isospin-color part of n and K^+ , $\psi(n)\psi(K^+)$, in terms of the successive coupling as follows (by omitting the isospin-triplet component):

$$\begin{aligned} [\psi(n)\psi(K^+)]_{\frac{1}{2}m} \rightarrow & -\frac{1}{\sqrt{2}}\frac{1}{\sqrt{2}} \left\{ \left(-\frac{1}{2}\chi_{(0\frac{1}{2}0)\frac{1}{2}m}^{\text{SC}} + \frac{\sqrt{3}}{2}\chi_{(0\frac{1}{2}1)\frac{1}{2}m}^{\text{SC}} \right) \xi_{(0\frac{1}{2}0)00}^{\text{SC}} \right. \\ & \left. + \left(-\frac{1}{2}\chi_{(1\frac{1}{2}0)\frac{1}{2}m}^{\text{SC}} + \frac{\sqrt{3}}{2}\chi_{(1\frac{1}{2}1)\frac{1}{2}m}^{\text{SC}} \right) \xi_{(1\frac{1}{2}0)00}^{\text{SC}} \right\} C_{((01)(00)(10))(00)000}^{\text{SC}}. \quad (26) \end{aligned}$$

Here the first $-\frac{1}{\sqrt{2}}$ factor comes from the Clebsch-Gordan coefficient of the isospin-singlet coupling and the second $\frac{1}{\sqrt{2}}$ factor from the symmetric spin-isospin function of the nucleon.

We briefly comment on the transformation of the orbital part. The coordinate appropriate for the diquark model is defined as

$$\begin{aligned} \mathbf{y}_1 &= \mathbf{r}_1 - \mathbf{r}_2, & \mathbf{y}_2 &= \mathbf{r}_3 - \mathbf{r}_4, & \mathbf{y}_3 &= \frac{1}{2}(\mathbf{r}_1 + \mathbf{r}_2) - \frac{1}{2}(\mathbf{r}_3 + \mathbf{r}_4), \\ \mathbf{y}_4 &= \frac{1}{4}(\mathbf{r}_1 + \mathbf{r}_2 + \mathbf{r}_3 + \mathbf{r}_4) - \mathbf{r}_5. \end{aligned} \quad (27)$$

An orbital function in the diquark model may be expressed as $\phi_{LM_L}(A', u', \mathbf{y})$. Because \mathbf{y} is related to \mathbf{x} by a linear transformation, $\mathbf{y} = T\mathbf{x}$, with an appropriate 4×4 matrix T , this orbital function can be reduced to the one in the \mathbf{x} representation:

$$\phi_{LM_L}(A', u', \mathbf{y}) = \phi_{LM_L}(A'_T, u'_T, \mathbf{x}), \quad (28)$$

with

$$A'_T = \tilde{T}A'T, \quad u'_T = \tilde{T}u'. \quad (29)$$

Here \tilde{T} is a transposed matrix of T . Therefore, we do not need to introduce a new diquark orbital function explicitly but can take into account it by simply adopting A'_T and u'_T as A and u in Eq. (8). It is clear that an orbital function appropriate for the baryon-meson model can be expressed in terms of the correlated Gaussian (8) as well.

It should be stressed that the present formalism can take into account all possible types of correlation in a single framework, so to evaluate matrix elements can be reduced to that in a particular representation [23]. That is, one does not need to calculate matrix elements separately in the different coordinate sets.

The calculation of matrix elements can be performed separately in the orbital, spin, isospin and color parts. The permutation P of the antisymmetrizer \mathcal{A} causes a linear transformation of the coordinate \mathbf{x} to \mathbf{x}' in the orbital function; $\mathbf{x}' = P\mathbf{x}$. Thus the matrix element of an operator \mathcal{O} acting in the orbital space can be calculated as

$$\langle \phi_{LM_L}(A, u, \mathbf{x}) | \mathcal{O} P | \phi_{L'M'_L}(A', u', \mathbf{x}) \rangle = \langle \phi_{LM_L}(A, u, \mathbf{x}) | \mathcal{O} | \phi_{L'M'_L}(\tilde{P}A'\tilde{P}, \tilde{P}u', \mathbf{x}) \rangle. \quad (30)$$

Here the action of the permutation results in just renaming A' as $\tilde{P}A'\tilde{P}$ and u' as $\tilde{P}u'$, so that we do not need to change the functional form of ϕ_{LM_L} at all. The orbital matrix element was evaluated using the method explained in detail in [23]. The matrix elements involving the spin, isospin and color functions are evaluated using the Wigner-Eckart theorem as well as SU(2) and SU(3) recoupling techniques [28].

III. RESONANCE IN A SINGLE-CHANNEL CALCULATION

The mass of the Θ^+ is in the continuum above the $N + K$ threshold. Here we briefly discuss how to predict a resonance mass using the basis functions explained in the previous section. There are some powerful methods such as a complex scaling method [30] and an analytic continuation in a coupling constant [31, 32] to use a generalization of bound-state problems for locating the resonance. We use the real stabilization method [21] among others for its simplicity. In the stabilization method the Schrödinger equation is solved in a box,

i.e., on a square-integrable basis, which makes all solutions look like bound states. From among the bound-state-looking discrete states, those corresponding to the resonances are singled out by exploiting their stability against changes of the box size (which is practically equivalent to the basis dimension in the present case).

We illustrate this procedure in a single-channel calculation where the basis functions are limited to one particular spin-isospin-color configuration. As the single channel we adopt two representative ones: One is the Jaffe-Wilczek model [9] in which both diquarks are restricted to $S=0, T=0, \Gamma=(01)$ and these identical bosons are coupled to be antisymmetric in the color state, and the other is the Karliner-Lipkin model [10] in which the triquark with $S=\frac{1}{2}, T=0, \Gamma=(10)$ and the diquark with $S=0, T=0, \Gamma=(01)$ are coupled to a color singlet state (see Eq. (25)). In the single-channel calculation, only the matrix A and the vector u are variational parameters characterizing the basis function, and the parameter space for them are first defined appropriately. Figure 1 plots the mass eigenvalues vs the basis dimension for $J^P = \frac{1}{2}^+$ ($L=1, S=\frac{1}{2}$) in the Jaffe-Wilczek model, where the basis was randomly chosen from the parameter space without any selection procedure and just increased one by one. A remarkable feature of this figure is that one has a solution whose mass stays nearly constant. The stable solution is not a ground state but has a large mass above the $N+K$ threshold. The rms radius calculated from the stable solution is also stable: The mass and the rms radius are 2370 MeV and 0.72 fm for the basis dimension $\mathcal{K}=100$, and 2340 MeV and 0.73 fm for $\mathcal{K}=200$, respectively. This stability is an indication required for the existence of a resonance. To extend this type of calculations to a full coupled-channels problem is hard, however, because the number of channels is fairly large. It is advisable to confirm the stability even though the basis dimension is truncated through some selection procedure.

Examples of such a truncated calculation are presented in Fig. 2 where the mass as well as the rms radius are displayed as a function of the basis dimension. Here the basis selection was performed using the SVM [22, 23] as it leads to virtually exact solutions in rather small dimension and its power is proved in diverse few-body problems. In the SVM the basis dimension is increased one by one by testing a number of candidates which are chosen randomly. The importance of each candidate is evaluated by calculating the energy gain

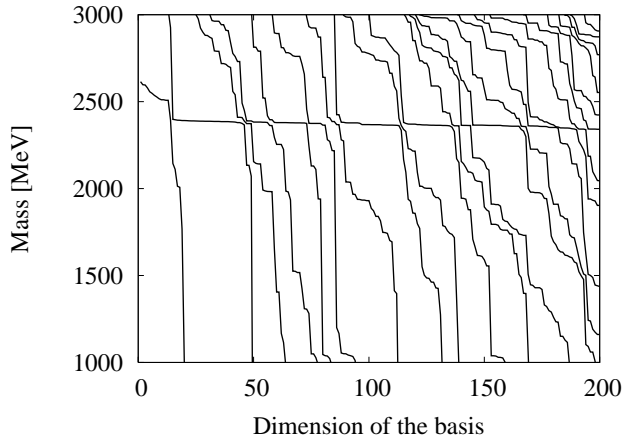


FIG. 1: The mass of the Θ^+ with $\frac{1}{2}^+$ on a random basis in the Jaffe-Wilczek model. The All potential is used.

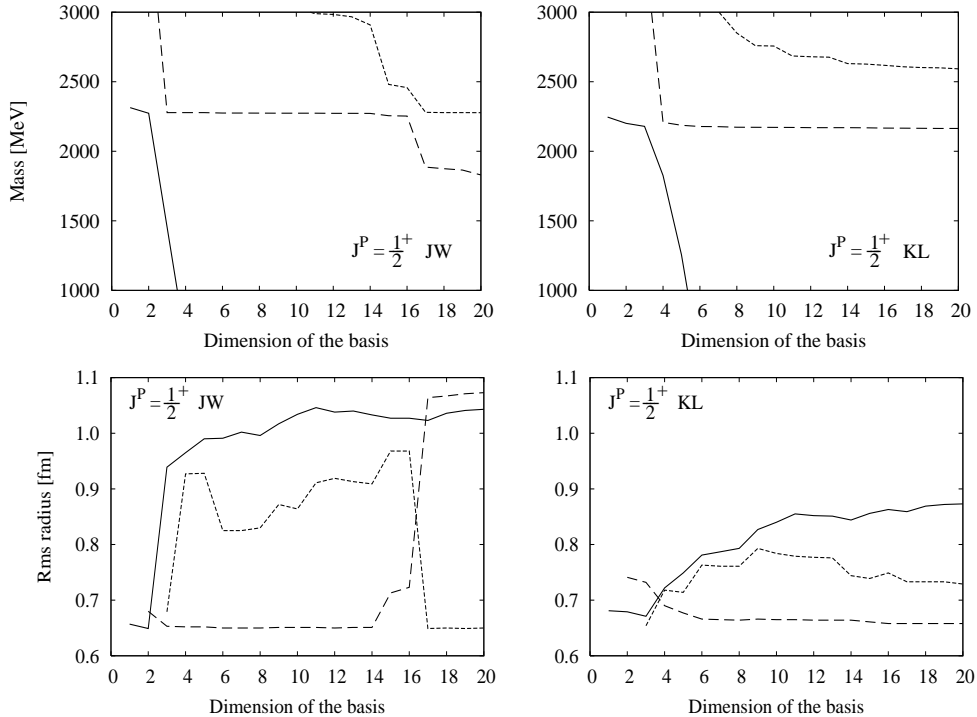


FIG. 2: The mass and rms radius of the Θ^+ in a single-channel calculation. The figures on the left side are the results in the Jaffe-Wilczek model, while those on the right side are obtained in the Karliner-Lipkin model. The AL1 potential is used.

produced when it is included in the basis set. The candidate which produces the lowest of the energies is chosen to be a member of the basis set. Furthermore, it is shown in [33] that the basis set for describing a resonance can be selected very efficiently with the SVM. The basis selection in the present calculation was actually done as follows: each element of A and u was randomly generated twenty times, and the best one among these trials was selected as a tentative candidate for a new basis. This process was repeated ten times to select a most successful one from among these tentative candidates. A typical computer time needed to determine twenty basis states was about half an hour on a computer loading the Intel (R) Pentium (R) 4 CPU 3.20 GHz.

We see two characteristics in either model of the figure. One is that the lowest mass decreases as the basis dimension increases, reaching even a negative value. The other is the appearance of such a unique mass eigenvalue that is stable against the increase of the basis dimension. By looking at the figure of the rms radius, we note that the radius corresponding to the former solution is rather large and continues to increase with increasing dimension. In contrast to this case, the radius for the latter solution stays approximately constant, and it decreases a little from the one of Fig. 1. According to the criterion of the real stabilization method, we may identify the latter mass as the resonance mass and the corresponding wave function as the approximate resonance wave function which is valid except at large distances. Of course the mass obtained here is just a result of the single-channel calculation, so before declaring it to be the Θ^+ mass we have to consider the effect of other channels which may contribute to the resonance. In particular, the effect of the NK channel must be examined carefully. This will be performed in the next section.

We have performed a single-channel calculation for the other configurations as well in each case of the successive coupling, the diquark model or the baryon-meson model. The falloff of the mass and the increase of the rms radius are observed in all the cases. The reason for this seems due to the color dependence of the quark-quark potential as was pointed out in sect. II A. First we notice that the mass of the colored subsystem happens to be negative and its radius gets very large obviously because of the $(\lambda_i^C \cdot \lambda_j^C)r_{ij}$ operator which works to deconfine the system in special color channels. A five-quark system usually contains such colored components, so the variational ground state will make use of it to gain the energy.

It is nevertheless fortunate that we have the sign of a resonance, that is, the stability in the mass diagram, which is indispensable for getting a resonance in the bound-state-looking calculations. Those cases which show the stability are characterized by that at least one of the diquarks is antisymmetric with respect to the simultaneous interchange of the spin, isospin and color degrees of freedom.

A single-channel calculation has also been performed for other J^P states. We have obtained some stable masses around 2500, 2700 and 2900 MeV for $(L=1, S=\frac{3}{2})$, $(L=2, S=\frac{1}{2})$ and $(L=2, S=\frac{3}{2})$ cases, respectively. It seems that the larger L and the larger S the system has the larger its mass is. This can be expected from the role played by the kinetic energy and the color magnetic piece of the quark-quark potential. We will focus our attention on the $J^P = \frac{1}{2}^\pm$ and $\frac{3}{2}^-$ states in what follows.

IV. RESULTS

A. Mass spectrum

We have made a coupled-channels calculation to predict the mass of the Θ^+ for $J^P = \frac{1}{2}^-$ ($L=0, S=\frac{1}{2}, T=0$), $\frac{1}{2}^+$ ($\frac{3}{2}^+$) ($L=1, S=\frac{1}{2}, T=0$) and $\frac{3}{2}^-$ ($L=0, S=\frac{3}{2}, T=0$). As discussed in sect. II B, there are in principle 30 channels for $S=\frac{1}{2}, T=0$ and 24 channels for $S=\frac{3}{2}, T=0$. Among these some channels play an important role to produce a resonance but some others play much less significant roles. In the actual calculation we first single out basis functions from those channels which give a stable mass in a single-channel calculation, and include them in the coupled-channels calculation. Included are 7, 5 and 12 channels for $J^P = \frac{1}{2}^-, \frac{3}{2}^-$ and $\frac{1}{2}^+ (\frac{3}{2}^+)$, respectively. These channels are expressed using the channel labels of $S_{12}, T_{12}, \Gamma_{12}, S_{34}, T_{34}, \Gamma_{34}, S_{1234}$ in the diquark model as follows:

$$\begin{aligned}
\text{for } J^P = \frac{1}{2}^- & \quad 00(01)00(01)0, 00(01)10(20)1, 01(20)11(01)1, 11(01)11(01)0, \\
& \quad 10(20)00(01)1, 11(01)01(20)1, 11(01)11(01)1, \\
\text{for } J^P = \frac{3}{2}^- & \quad 10(20)00(01)1, 11(01)01(20)1, 00(01)10(20)1, 01(20)11(01)1, \\
& \quad 11(01)11(01)1, \\
\text{for } J^P = \frac{1}{2}^+ & \quad 00(01)00(01)0, 00(01)10(20)1, 01(20)11(01)1, 11(01)11(01)0, \\
& \quad 10(20)00(01)1, 11(01)01(20)1, 10(01)10(20)1, 10(20)10(01)1, \\
& \quad 11(01)11(01)1, 11(20)11(01)1, 10(01)00(01)1, 00(01)10(01)1. \quad (31)
\end{aligned}$$

To obtain a final result for a resonance, we further consider the effect of those basis functions which are generated from the NK channel for $J^P = \frac{1}{2}^\pm$ or from the NK^* channel for $\frac{3}{2}^-$ because the coupling of the resonance with that channel appears to be important for

calculating the width. Note that the NK channel does not couple to $\frac{3}{2}^-$ states as they differ in the total spin S , but the NK^* channel can have the same spin $S = \frac{3}{2}$. For example, the NK channel basis functions included are expressed as

$$\Phi_i(NK) = \mathcal{A} \left\{ \left[[\Psi_{\frac{1}{2}\frac{1}{2}}(N)\Psi_{0\frac{1}{2}}(K)]_{I=\frac{1}{2}T=0} \exp\left(-\frac{1}{2}a_i z_4^2\right) \mathcal{Y}_\ell(z_4) \right]_{JM} \right\}, \quad (32)$$

where $\Psi_{I=\frac{1}{2}T=\frac{1}{2}}(N)$ and $\Psi_{I=0T=\frac{1}{2}}(K)$ are respectively the wave functions of N and K which are obtained by solving the three-quark and quark-antiquark Hamiltonians with the potential of Eq. (2) or Eq. (3). These are coupled to the relative motion function of Gaussian form with the orbital angular momentum ℓ to the total angular momentum JM . Here the coordinate $\mathbf{z}_4 = \mathbf{R}_N - \mathbf{R}_K$ is the relative distance vector between the center of mass of N , \mathbf{R}_N , and the center of mass of K , \mathbf{R}_K . In the calculation the length parameter is set to be $1/\sqrt{a_i} = 0.6 \times 1.4^{i-1}$ fm ($i = 1, 2, \dots, 5$).

The Hamiltonian is diagonalized in the set of the chosen basis functions. Figures 3 and 4 display the calculated mass as a function of the basis dimension. We clearly see a

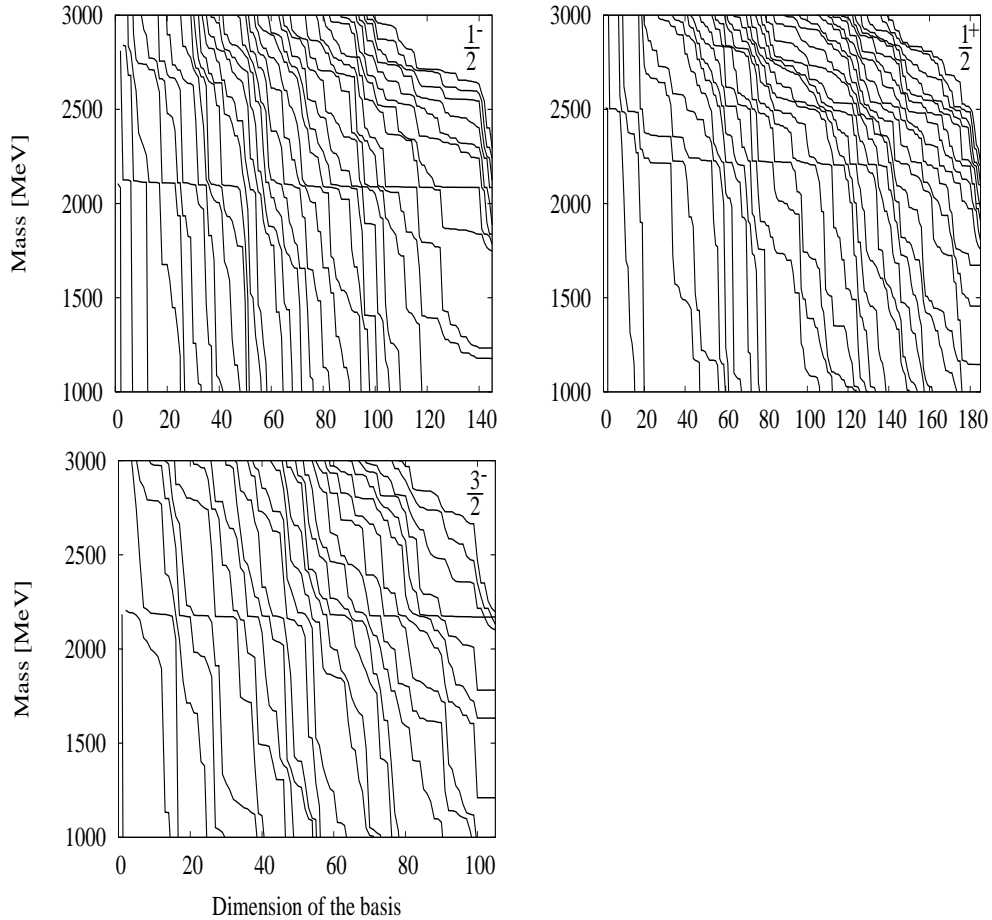


FIG. 3: The mass of the Θ^+ in a coupled-channels calculation. The NK channel is explicitly included for $J^P = \frac{1}{2}^\pm$, while the NK^* channel is for $\frac{3}{2}^-$. The AL1 potential is used.

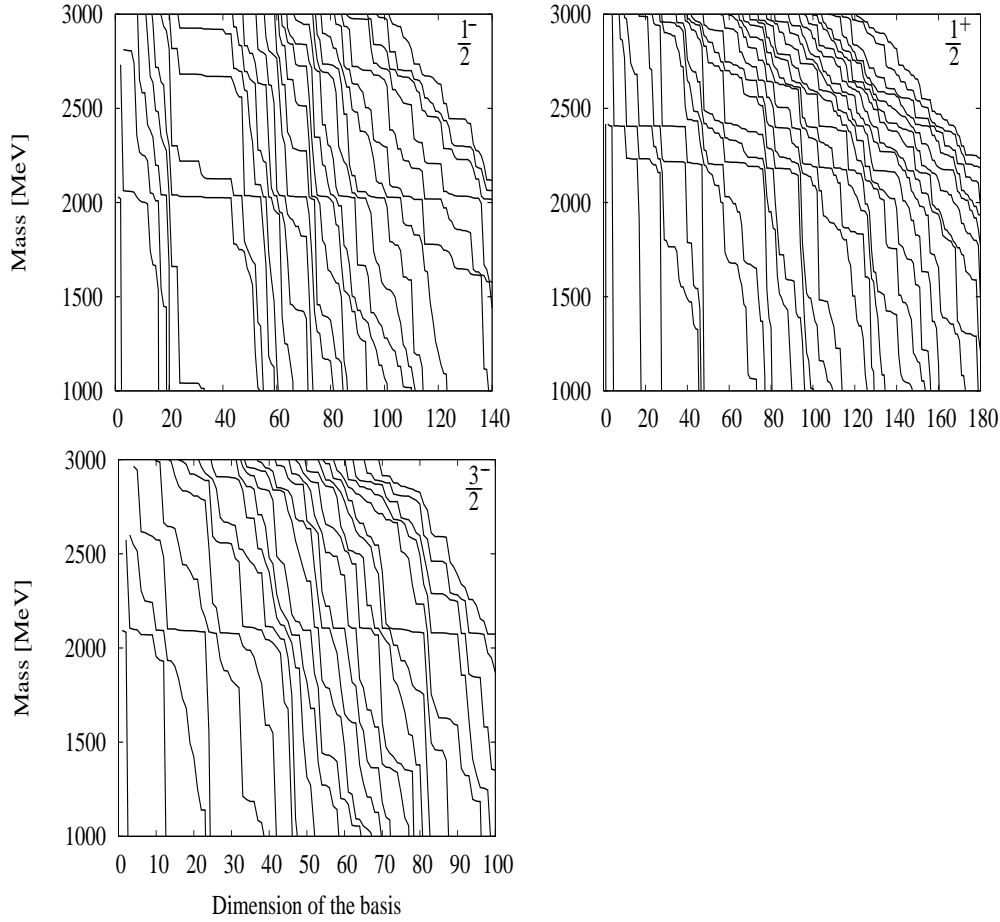


FIG. 4: The same as Fig. 3 but for the TS potential.

stabilized mass in the diagram and have confirmed that the rms radius calculated from the corresponding wave function is stable. This stabilized solution is accepted as a resonance we seek. We have found that the mass and the radius of the stabilized solution remains basically unchanged by including the NK (and NK^*) channel of Eq. (32). Evidently, our resonance does not correspond to a variational energy minimum. We have used a variational method in order to set up compact, appropriate basis functions. This is in contrast to the approach in [11, 12], where a variational energy minimum is looked for and moreover a coupling to the baryon-meson channel like NK is excluded from the model space.

The masses and rms radii obtained in the present calculation are summarized in Fig. 5 and Table IV. It is concluded that the mass of the Θ^+ increases in order of $J^P = \frac{1}{2}^-, \frac{3}{2}^-, \frac{1}{2}^+(\frac{3}{2}^+)$, which agrees with the result of Ref. [11]. A lower mass is obtained for the $\frac{1}{2}^-$ state than for the $\frac{1}{2}^+$ state, which is consistent with the recent variational Monte carlo calculation [13] but is opposite to the level order obtained in [14]. The color magnetic and kinetic energy terms in the Hamiltonian play the most important contribution to generate the mass differences. The mass splitting between the $\frac{3}{2}^-$ and $\frac{1}{2}^+(\frac{3}{2}^+)$ states is smaller in the AL1 potential than that in the TS potential, but both potentials otherwise give qualitatively similar results. Our result for the TS potential is compared to that of [11], and we see that the mass splitting is

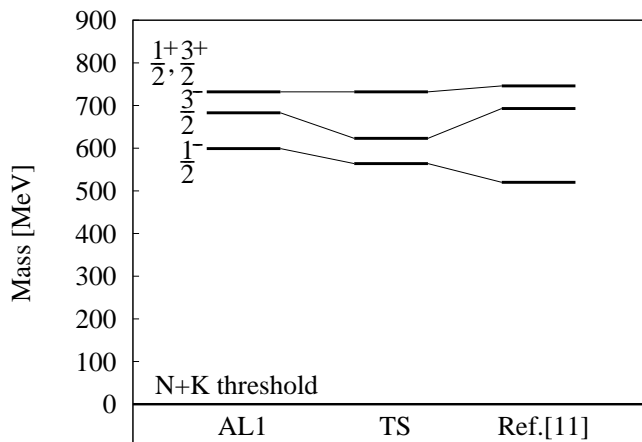


FIG. 5: The mass spectrum of the Θ^+ from the $N+K$ threshold. The result of Ref. [11] is due to the TS potential.

not necessarily the same between the two. This is probably due to the difference in obtaining the mass as well as in specifying the correlation of the quark dynamics.

The calculated mass of the Θ^+ is higher than the observed mass (~ 1540 MeV) by about 500-600 MeV. This appears to be common in all the calculations using the potential of OGE type [11, 12, 14] or the OGE plus one-pion exchange potential [13]. The zero-point energy term is uncertain, so it is hard to get an absolute mass unambiguously. There are some discussions to reduce the mass. One is to consider the flavor-spin dependence of the quark-quark potential or the one-boson exchange potential [15, 17]. The second is to take into account the role of the instanton induced interaction [34, 35]. Though this interaction is expected to bring about an extra attraction, its effect has not yet been quantified. The third is to consider the relativistic effect of the quark motion. An extensive calculation has been made in [11] which used the semirelativistic expression for the kinetic energy and the one-boson exchange potential as well as the OGE potential. It seems that the $\frac{1}{2}^+$ state comes down close to or even lower than the $\frac{3}{2}^-$ state. The calculated mass is, however, still larger than the observed mass, and even goes around 2 GeV if the zero-point energy is taken to be proportional to the number of quarks.

TABLE IV: The mass and rms radius of the Θ^+ . The calculated $N+K$ threshold energy is 1486 MeV for the AL1 potential and 1451 MeV for the TS potential, respectively.

J^P	AL1		TS	
	M [MeV]	$\sqrt{\langle r^2 \rangle}$ [fm]	M [MeV]	$\sqrt{\langle r^2 \rangle}$ [fm]
$\frac{1}{2}^-$	2086	0.57	2015	0.63
$\frac{3}{2}^-$	2169	0.59	2074	0.63
$\frac{1}{2}^+, \frac{3}{2}^+$	2219	0.74	2183	0.72

B. Decay width and spin-parity

The width of a resonance is in principle calculated through a coupling to the continuum states of decay channels. As we have localized the Θ^+ , it may be appealing to use, for example, the complex scaling method to calculate the width as was done in [33]. This is, however, too sophisticated in the present case since the calculated Θ^+ mass is subject to large uncertainty of the quark-quark potential. On the other hand, the wave function of the resonance remains the same for an arbitrary adjustment of the resonance energy due to the change of the zero-point energy term, so we instead use the R -matrix theory [36, 37] in which the width Γ of an isolated resonance is calculated through

$$\Gamma = 2P_\ell(a)\gamma^2(a), \quad (33)$$

where a is a channel radius and $P_\ell(a)$ is the penetrability given by

$$P_\ell(a) = \frac{ka}{j_\ell^2(ka) + n_\ell^2(ka)}. \quad (34)$$

Here ℓ and k are the orbital angular momentum and the wave number of the relative motion between the decaying particles, and j_ℓ and n_ℓ are the spherical Bessel functions. When both of the decaying particles are charged, the spherical Bessel functions should be replaced by the Coulomb functions.

Most crucial in Eq. (33) is the reduced width $\gamma^2(a)$, which is related to the reduced width amplitude $y(a)$ for the decay to a baryon B and a meson M :

$$\begin{aligned} \gamma^2(a) &= \frac{a}{2\mu}y^2(a), \\ y(r) &= \sqrt{\frac{4!}{3!}} \left\langle \left[[\Psi_{I_B T_B}(B)\Psi_{I_M T_M}(M)]_{I T M T} Y_\ell(\widehat{\mathbf{z}}_4) \right]_{JM} \frac{\delta(z_4 - r)}{z_4 r} \right| \Psi_{JM}^P \rangle. \end{aligned} \quad (35)$$

Here μ is the reduced mass of the baryon and the meson, $\Psi_{I_B T_B}(B)$ is the baryon wave function which is properly antisymmetrized and normalized, and $\Psi_{I_M T_M}(M)$ is the normalized meson wave function. The coordinate \mathbf{z}_4 is the relative distance vector between the baryon's center of mass and the meson's center of mass. Introducing a complete basis set $\{f_{n\ell}(r)Y_{\ell m}(\hat{\mathbf{r}})\}$, the calculation of $y(r)$ is reduced to that of the overlap:

$$y(r) = \sqrt{\frac{4!}{3!}} \sum_n f_{n\ell}(r) \left\langle \left[[\Psi_{I_B T_B}(B)\Psi_{I_M T_M}(M)]_{I T M T} f_{n\ell}(z_4) Y_\ell(\widehat{\mathbf{z}}_4) \right]_{JM} \right| \Psi_{JM} \rangle. \quad (36)$$

Figure 6 displays the reduced width amplitude of the Θ^+ resonance obtained with the AL1 potential. The spins of the decay channel are taken as $(I, \ell) = (\frac{1}{2}, 0)$ for $J^P = \frac{1}{2}^-$ and $(I, \ell) = (\frac{1}{2}, 1)$ for $J^P = \frac{1}{2}^+$ ($\frac{3}{2}^+$), respectively. Note that the Θ^+ with $J^P = \frac{3}{2}^-$ cannot decay to the nK^+ channel because it has $S = \frac{3}{2}$ and its reduced width amplitude to that channel vanishes. For it to decay to the nK^+ channel, one has to take into account tensor components of the interaction between the quarks. However, the $\frac{3}{2}^-$ state can decay to the nK^{*+} channel, so the reduced width amplitude for this decay with $(I, \ell) = (\frac{3}{2}, 0)$ is displayed in the figure. It is found that the reduced width amplitude hardly changes with the inclusion of the NK (or NK^*) channel basis functions defined in Eq. (32). The amplitude of the Wigner limit

(WL), $y(r) = \sqrt{\frac{3}{r^3}}$, is also plotted in the figure. The Wigner limit is the partial width of a particular state whose wave function is uniform up to r and zero beyond, and it is a measure to judge whether the resonance has a large component in the decay channel or not. Since the calculated reduced width amplitudes are considerably small compared to the Wigner limit, we can conclude that the Θ^+ does not have large nK^+ component. This point will be confirmed in sect. IV C. It is noted that the amplitude of the $\frac{3}{2}^-$ state is especially small at $r \geq 1$ fm.

We estimate the following decay width according to Eq. (33): the nK^+ decay of the Θ^+ with $\frac{1}{2}^\pm$ and the nK^{*+} decay of the Θ^+ with $\frac{3}{2}^-$. Because the calculated mass is subject to change due to the uncertainty of precise knowledge on the interaction between the quarks, we display in Fig. 7 the width as a function of the decay energy E . The channel radius a relevant to the decay is estimated as a sum of their radii, and it is about 1.1 fm using the values of Table I. The channel radius dependence is also presented around $a=1$ fm.

First let us accept the calculated mass as it is. Then we conclude that no pentaquark states Θ^+ appear around 1540 MeV, but their masses are expected to be larger than 2 GeV. The decay width is then very large, which is different from the conclusion of [14]. Even for the $\frac{1}{2}^+$ state, the width would be in the order of 100 MeV. In the case of $J^P = \frac{3}{2}^-$, the mass from the $n+K^{*+}$ threshold is 270 MeV for the AL1 potential and 320 MeV for the TS potential, respectively, so that the decay width to this channel is a few MeV. The magnitude of this width is probably small enough to be observed as a sharp resonance.

Next let us assume that, by shifting the calculated mass spectrum, one of the calculated Θ^+ resonances corresponds to the observed mass, 1540 MeV, namely 100 MeV above the $n+K^+$ threshold. There are following three possibilities, and we estimate the decay width from Fig. 7 for each case:

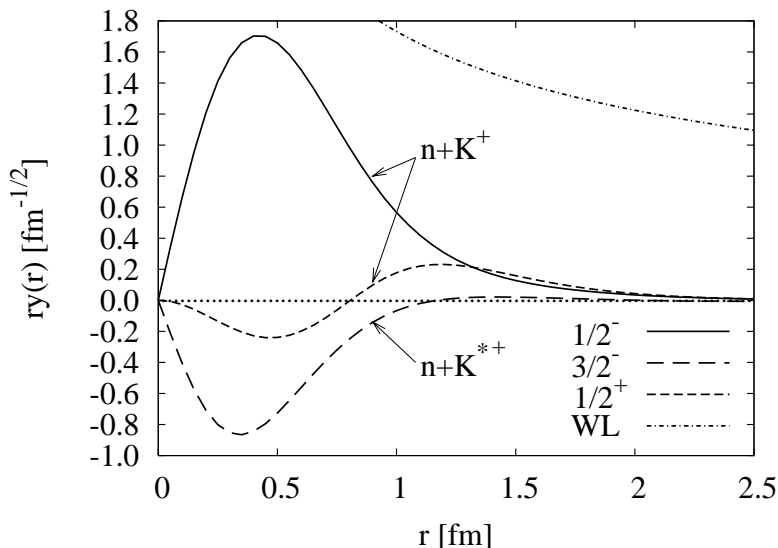


FIG. 6: The reduced width amplitude of the Θ^+ to the nK^+ channel for $J^P = \frac{1}{2}^\pm$ and to the nK^{*+} channel for $J^P = \frac{3}{2}^-$. The reduced width amplitude for $J^P = \frac{3}{2}^+$ is the same as that for $J^P = \frac{1}{2}^+$. The AL1 potential is used.

- (1) If the spin-parity of the Θ^+ is $\frac{1}{2}^-$, its width is several tens to 100 MeV, which is too large to be compared to the observation.
- (2) If the spin-parity of the Θ^+ is $\frac{3}{2}^-$, its nK^+ decay width is practically zero. Because of the mass spectrum predicted by the present model (see Fig 5), another Θ^+ with $\frac{1}{2}^-$ is expected to appear below the $\Theta^+(\frac{3}{2}^-)$ as well and its width is in the order of a few MeV.
- (3) If the spin-parity of the Θ^+ is $\frac{1}{2}^+(\frac{3}{2}^+)$, its nK^+ decay width is about 10 MeV. Below this resonance other Θ^+ states with $\frac{1}{2}^-$ and $\frac{3}{2}^-$ appear as quasi-bound states.

The case (1) is apparently in contradiction to experiment. The case (2) may remain as an actual possibility because the decay width is practically zero. However, in this case another pentaquark state with $J^P = \frac{1}{2}^-$ with a small width should also be observed near or slightly above the $n+K^+$ threshold. No such experimental information is available at present. The case (3) can also be an actual possibility and the decay width is in the order of 10 MeV. Though the existence of the Θ^+ states with $\frac{1}{2}^-$ and $\frac{3}{2}^-$ are also predicted in this case, their

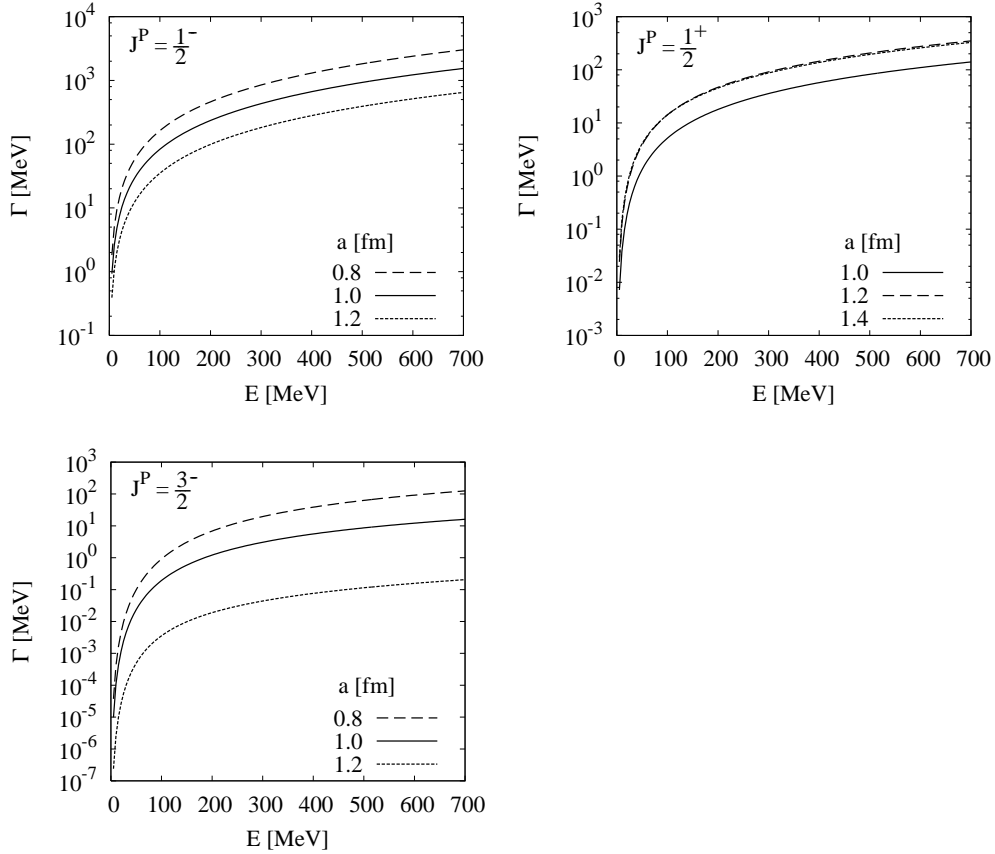


FIG. 7: The decay width Γ of the Θ^+ to the nK^+ channel for $J^P = \frac{1}{2}^\pm$ and to the nK^{*+} channel for $J^P = \frac{3}{2}^-$. E is the decay energy from the respective threshold and a is the channel radius. The AL1 potential is used.

energies are below the $n+K^+$ threshold. Thus we expect no signal for the existence of such states from the type of experiment which uses the K^+n invariant mass spectrum for identifying the pentaquark. Therefore, the case (3) that the spin-parity of the $\Theta^+(1540)$ is $\frac{1}{2}^+$ ($\frac{3}{2}^+$) seems not to be in contradiction with the available experimental information.

C. Structure

To discuss the structure of the Θ^+ , it is useful to calculate a single-particle density and a correlation function between the particles. These functions F are all defined as

$$F(\mathbf{r}) = \langle \Psi_{JM}^P | \delta(\tilde{\omega}\mathbf{x} - \mathbf{r}) | \Psi_{JM}^P \rangle, \quad (37)$$

where $\omega = (\omega_1, \omega_2, \omega_3, \omega_4)$ is a vector which is chosen appropriately depending on the quantity of interest. For example, the density distribution of the ud quarks from the center of mass $\mathbf{R}_{\text{c.m.}}$ of the system, the quark-quark correlation function and the quark-antiquark (\bar{s}) correlation function can be calculated by choosing $\omega = (0, 0, -\frac{3}{4}, \frac{m_s}{4m_{ud}+m_s})$ ($\tilde{\omega}\mathbf{x} = \mathbf{r}_4 - \mathbf{R}_{\text{c.m.}}$), $\omega = (1, 0, 0, 0)$ ($\tilde{\omega}\mathbf{x} = \mathbf{r}_1 - \mathbf{r}_2$), and $\omega = (0, 0, -\frac{3}{4}, 1)$ ($\tilde{\omega}\mathbf{x} = \mathbf{r}_4 - \mathbf{r}_5$), respectively, because the wave function is properly antisymmetrized. The choice of $\omega = (0, 0, 0, 1)$ gives the distribution ($q^4\bar{s}$) of the \bar{s} from the center of mass of the four quarks. When the delta function, $\delta(\tilde{\omega}\mathbf{x} - \mathbf{r})$, is expanded in multipoles, only the monopole term contributes to the function $F(\mathbf{r})$ for both cases of $J^P = \frac{1}{2}^\pm$, so $F(\mathbf{r})$ becomes spherically symmetric.

Figure 8 displays the density distributions as well as the correlation functions for the Θ^+ with $J^P = \frac{1}{2}^-$. It is seen that the distribution of the \bar{s} is confined in the smaller region around the center of mass of the system than the ud -quark distribution. The probability density reaches a maximum at about 0.30 fm for \bar{s} and about 0.44 fm for ud , respectively. This feature seems to arise from the fact that the quark-antiquark interaction is stronger than the quark-quark interaction. Corresponding to this feature, we see from the correlation function that the average distance between the ud and \bar{s} quarks is shorter than that between the ud quarks. Figure 9 displays the similar distributions for the Θ^+ with $\frac{1}{2}^+$. The distribution

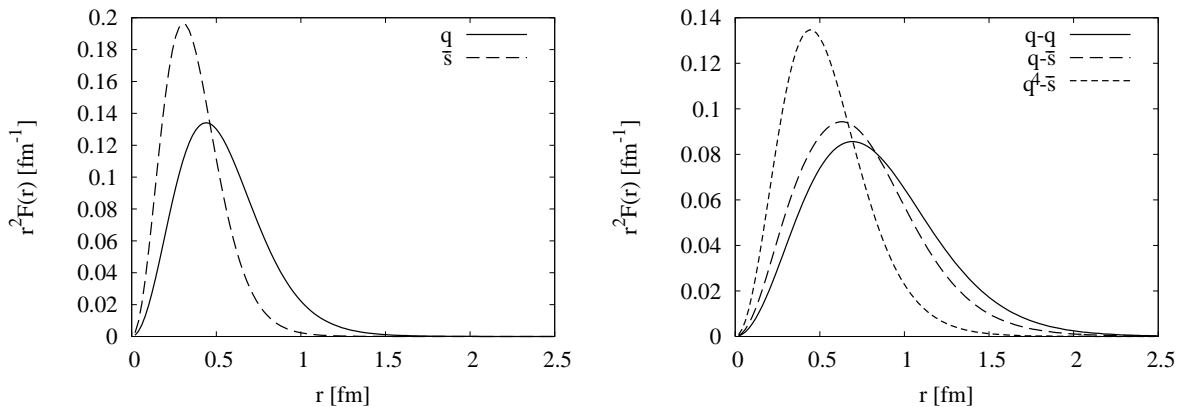


FIG. 8: The density distributions of the quarks (left) and the correlation functions between the quarks (right) for the Θ^+ with $J^P = \frac{1}{2}^-$. The AL1 potential is used.

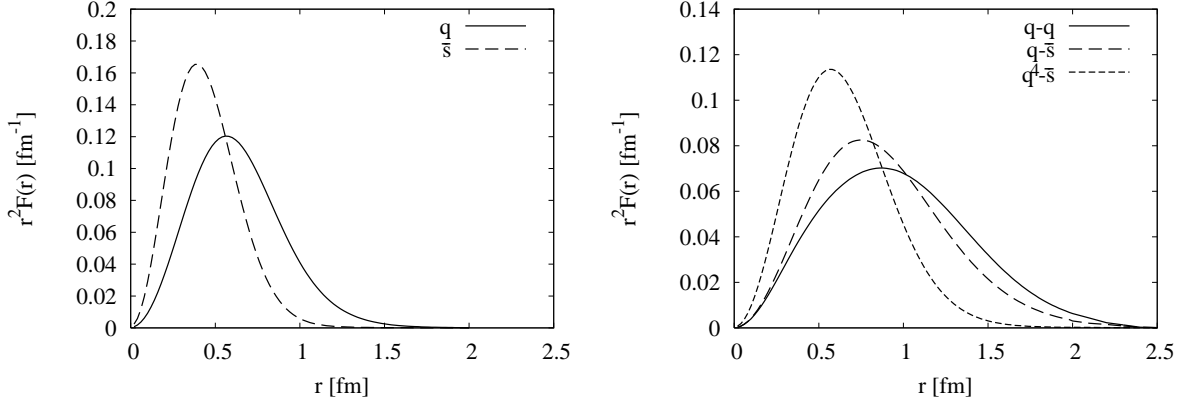


FIG. 9: The same as Fig. 8 but for $J^P = \frac{1}{2}^+$.

extends to larger distances than that of $J^P = \frac{1}{2}^-$. Again, the \bar{s} distribution has a peak at smaller distances from the center of mass than the ud distribution.

Another structure information is obtained by decomposing the wave function into various channels of the spin, isospin and color spaces. To this end, let us define the channel wave function Φ_c . See sects. II B and II C. In the diquark-diquark decomposition Φ_c is defined as

$$\Phi_{cM_S} = \frac{1}{\sqrt{2(1 + \delta_{12,34})}} \left\{ \chi_{(S_{12}S_{34}S_{1234})SM_S}^{\text{DD}} \xi_{(T_{12}T_{34}0)00}^{\text{DD}} C_{(\Gamma_{12}\Gamma_{34}(10))(00)000}^{\text{DD}} \right. \\ \left. + \pi \sigma \chi_{(S_{34}S_{12}S_{1234})SM_S}^{\text{DD}} \xi_{(T_{34}T_{12}0)00}^{\text{DD}} C_{(\Gamma_{34}\Gamma_{12}(10))(00)000}^{\text{DD}} \right\}, \quad (38)$$

where $\delta_{12,34} = \delta_{S_{12}S_{34}} \delta_{T_{12}T_{34}} \delta_{\Gamma_{12}\Gamma_{34}}$, and σ is the phase defined by

$$\sigma = (-1)^{S_{12}+S_{34}-S_{1234}+T_{12}+T_{34}+\lambda_{12}+\lambda_{34}+\mu_{12}+\mu_{34}-1}. \quad (39)$$

The channel index c is characterized by a set of values $(S_{12}, T_{12}, \Gamma_{12}, S_{34}, T_{34}, \Gamma_{34}, S_{1234}, \pi)$, where $\pi = \pm 1$ determines the parity of the Φ_c . The Φ_c with $\pi = +1$ is symmetric with respect to the simultaneous interchange of the spin, isospin and color parts of the two diquarks, and the Φ_c with $\pi = -1$ is antisymmetric. In the case of $\delta_{12,34} = 1$, a combination of $\pi\sigma = 1$ only is possible, that is, either $\pi = +1$ or $\pi = -1$ is allowed depending on whether $S_{1234} = 1$ or $S_{1234} = 0$. In the baryon-meson decomposition Φ_c is defined as

$$\Phi_{cM_S} = \chi_{(S_{12}S_{123}S_{45})SM_S}^{\text{BM}} \xi_{(T_{12}T_{123}\frac{1}{2})00}^{\text{BM}} C_{(\Gamma_{12}\Gamma_{123}\Gamma_{45})(00)000}^{\text{BM}}. \quad (40)$$

Here the channel index c stands for $(S_{12}, T_{12}, \Gamma_{12}, S_{123}, T_{123}, \Gamma_{123}, S_{45}, \Gamma_{45})$. In particular, the NK channel wave function is defined as

$$\Phi_{NK M_S} = \frac{1}{\sqrt{2}} \left\{ \chi_{(0\frac{1}{2}0)\frac{1}{2}M_S}^{\text{BM}} \xi_{(0\frac{1}{2}\frac{1}{2})00}^{\text{BM}} + \chi_{(1\frac{1}{2}0)\frac{1}{2}M_S}^{\text{BM}} \xi_{(1\frac{1}{2}\frac{1}{2})00}^{\text{BM}} \right\} C_{((01)(00)(00))(00)000}^{\text{BM}}. \quad (41)$$

The probability $P_c(J^P)$ of finding the channel c in the Θ^+ is calculated as the expectation value of the projector $\sum_{M_S} |\Phi_{cM_S}\rangle \langle \Phi_{cM_S}|$:

$$P_c(J^P) = \sum_{M_S} \langle \Psi_{JM}^P | \Phi_{cM_S}\rangle \langle \Phi_{cM_S} | \Psi_{JM}^P\rangle. \quad (42)$$

Values of $P_c(\frac{1}{2}^\pm)$ are listed in Table V for the diquark model and in Table VI for the baryon-meson model. The channel of the first row in Table V represents the diquark model of Jaffe-Wilczek [9]. It is seen that this channel occupies a relatively large component in the $\frac{1}{2}^+$ state as expected but its magnitude is not overwhelmingly large. Following this channel, the diquark pair with $S_{12}T_{12}\Gamma_{12} = 11(01)$ and $S_{34}T_{34}\Gamma_{34} = 11(20)$ occupies a significant weight for $J^P = \frac{1}{2}^+$. The channel of the third row corresponds to that of the diquark-triquark model [10] as shown in Eq. (25). We see that the configuration of the Karliner-Lipkin model is dominating in the $\frac{1}{2}^-$ state but it is not a main configuration in the $\frac{1}{2}^+$ state. With the probability of more than 80 %, the two diquarks in the $\frac{1}{2}^-$ state are found in either the Karliner-Lipkin channel or the channel with $S_{12}T_{12}\Gamma_{12} = 11(01)$, $S_{34}T_{34}\Gamma_{34} = 11(01)$, $S_{1234} = 1$. It is seen from Table VI that the components in the baryon-meson decomposition are spread over many channels. Relatively large components do not necessarily appear in colorless baryons. The probability summed over the colored baryon-meson channels is 67 %, which signals the importance of the hidden color components. The NK component, $P_{NK}(J^P)$, is calculated to be 0.14 for the $\frac{1}{2}^-$ state and 0.073 for the $\frac{1}{2}^+$ state, respectively. The magnitude of this channel is related to the reduced width to the nK^+ channel discussed in sect. IV B, and it is certainly small, especially for the $\frac{1}{2}^+$ state.

V. SUMMARY

We have studied the mass and the decay width of the Θ^+ consisting of $uudd\bar{s}$ quarks in the constituent quark model. The quarks are assumed to interact via a variant of the one-gluon exchange potential plus a phenomenological confinement potential which reproduce the masses of e.g., N , K and K^* reasonably well. The five-quark states are described using the correlated Gaussian basis together with the general spin-isospin-color wave functions. The basis functions are set up with the stochastic variational method. One of the advantages of the present approach is that the importance of all the possible color configurations can be tested, so that the hidden color components are naturally taken into account in the calculation. We have performed coupled-channels calculations to predict the Θ^+ masses for $J^P = \frac{1}{2}^- (L = 0, S = \frac{1}{2}, T = 0)$, $\frac{1}{2}^+ (\frac{3}{2}^+) (L = 1, S = \frac{1}{2}, T = 0)$ and $\frac{3}{2}^- (L = 0, S = \frac{3}{2}, T = 0)$. The NK and NK^* channels are explicitly included as they are expected to be important to obtain the decay width. The real stabilization method is successfully used to locate the resonance in the continuum states above the $N+K$ threshold. The ground state is found to be $\frac{1}{2}^-$ and its mass is about 2 GeV, which is 500-600 MeV higher than the observed value. The first and second excited states are $\frac{3}{2}^-$ and $\frac{1}{2}^+ (\frac{3}{2}^+)$. The color magnetic and kinetic energy terms of the Hamiltonian are the most important pieces which contribute to this level ordering.

To estimate the decay width of the Θ^+ , we have used the R -matrix theory in which most crucial is the reduced width amplitude for the relevant decay channel. The decay channel is specified by the angular momentum I , the addition of the spins of the baryon and the meson, as well as the relative orbital angular momentum ℓ between them. The calculated decay width is the nK^+ decay with $(I, \ell) = (\frac{1}{2}, 0)$ for $\frac{1}{2}^-$ and $(I, \ell) = (\frac{1}{2}, 1)$ for $\frac{1}{2}^+ (\frac{3}{2}^+)$, respectively. For the Θ^+ with $J^P = \frac{3}{2}^-$, the decay to the nK^+ channel is forbidden because the corresponding reduced width amplitude vanishes, so the decay width to the nK^{*+} channel is calculated. All the reduced width amplitudes are small compared to the Wigner limit value. As the mass of the Θ^+ is very large compared to the threshold, the decay

width becomes very broad except for the $\frac{3}{2}^-$ state whose decay width to the nK^{*+} channel is only a few MeV. We have also estimated the decay width by shifting the calculated mass to the observed mass, i.e., 100 MeV above the $n+K$ threshold. This shift causes no change in the resonance wave functions. The possibility that the observed state is $\frac{1}{2}^-$ is ruled out because its width is still too large. The case that it is either $\frac{3}{2}^-$ or $\frac{1}{2}^+$ ($\frac{3}{2}^+$) appears not to be inconsistent with the observation of the small width. However, in both cases other pentaquark state with different J^P is expected to exist below the observed one at 1540 MeV. Its experimental confirmation will give us a support for the Θ^+ .

The structure of the $\frac{1}{2}^\pm$ states is discussed through the density distributions of ud and \bar{s} quarks as well as the two-particle correlation functions of the quarks. It is found that the \bar{s} quark has a narrower distribution near the center of mass of the $uudd$ quarks than the ud quark. The average $q-q$ distance is longer compared to that of $q-\bar{s}$. These characteristics can be understood from the fact that the $q-\bar{q}$ interaction is stronger than the $q-q$ interaction. We have decomposed the resonance wave function into various components using the diquark-diquark model and the baryon-meson model. The baryon-meson configuration of the Karliner-Lipkin model is in fact a main component in the $\frac{1}{2}^-$ state but not an important component in the $\frac{1}{2}^+$ state, differing from its expectation. In contrast to this, the diquark-diquark configuration of the Jaffe-Wilczek model occupies the largest component in the $\frac{1}{2}^+$ state as expected, but its magnitude is not very large. The components are actually spread over many diquark-diquark channels.

Acknowledgments

This work was in part supported by a Grant-in-Aid for Scientific Research (No. 14540249) of the Japan Society for the Promotion of Science and a Grant for Promotion of Niigata University Research Projects (2005-2007).

-
- [1] A. De Rújula, H. Georgi and S. L. Glashow, Phys. Rev. D **12** (1975) 147.
 - [2] B. Silvestre-Brac, Few-Body Systems **20** (1996) 1.
 - [3] D. Diakonov, V. Petrov and M. Polyakov, Z. Phys. A **359** (1997) 305.
 - [4] T. Nakano *et al.*, Phys. Rev. Lett. **91** (2003) 012002.
 - [5] S. Stepanyan *et al.*, Phys. Rev. Lett. **91** (2003) 252001.
 - [6] J. Barth *et al.*, Phys. Lett. B **572** (2003) 127.
 - [7] K. H. Hicks, Prog. Nucl. Part. Phys. **55** (2005) 647.
 - [8] M. I. Adamovich *et al.*, Phys. Rev. C **72** (2005) 055201.
 - [9] R. Jaffe and F. Wilczek, Phys. Rev. Lett. **91** (2003) 232003.
 - [10] M. Karliner and H. J. Lipkin, Phys. Lett. B **575** (2003) 249.
 - [11] S. Takeuchi and K. Shimizu, Phys. Rev. C **71** (2005) 062202(R) and Ref. 16 cited therein.
 - [12] Y. Kanada-En'yo, O. Morimatsu and T. Nishikawa, Phys. Rev. C **71** (2005) 045202.
 - [13] M. W. Paris, Phys. Rev. Lett. **95** (2005) 202002.
 - [14] E. Hiyama, M. Kamimura, A. Hosaka, H. Toki and M. Yahiro, Phys. Lett. **B**, to be published. (hep-ph/0507105).
 - [15] Fl. Stancu and D. O. Riska, Phys. Lett. B **575** (2003) 242.

- [16] M. Oka, Prog. Theor. Phys. **112** (2004) 1.
- [17] C. E. Carlson, C. D. Carone, H. J. Kwee and V. Nazaryan, Pys. Rev. D **70** (2004) 037501.
- [18] A. Hosaka, M. Oka and T. Shinozaki, Phys. Rev. D **71** (2005) 074021.
- [19] P. Bicudo and G. M. Marques, Phys. Rev. D **69** (2004) 011503(R).
- [20] F. J. Llanes-Estrada, E. Oset and V. Mateu, Phys. Rev. C **69** (2004) 055203.
- [21] A. U. Hazi and H. S. Taylor, Phys. Rev. A **1** (1970) 1109.
- [22] K. Varga and Y. Suzuki, Phys. Rev. C **52** (1995) 2885.
- [23] Y. Suzuki and K. Varga, *Stochastic Variational Approach to Quantum-Mechanical Few-Body Problems* (Springer, Berlin, 1998).
- [24] J. P. Elliott, Proc. R. Soc. A **245** (1958) 128, 562.
- [25] L. Ya. Glozman and D. O. Riska, Phys. Rep. **268** (1996) 263.
- [26] L. Ya. Glozman, Z. Papp, W. Plessas, K. Varga and R. F. Wagenbrunn, Phys. Rev. C **57** (1998) 3406.
L. Ya. Glozman, W. Plessas, K. Varga and R. F. Wagenbrunn, Phys. Rev. D **58** (1998) 094030.
- [27] Y. Suzuki, J. Usukura and K. Varga, J. Phys. B **31** (1998) 31.
- [28] K. T. Hecht, Nucl. Phys. **62** (1965) 1.
- [29] J. P. Draayer and Y. Akiyama, J. Math. Phys. **14** (1973) 1904.
- [30] J. Aguilar and J. M. Combes, Commun. Math. Phys. **22** (1971) 269.
E. Balslev and J. M. Combes, Commun. Math. Phys. **22** (1971) 280.
- [31] V. I. Kukulin and V. M. Krasnopol'sky, J. Phys. A **10** (1977) 33.
V. I. Kukulin, V. M. Krasnopol'sky and M. Miselkhi, Sov. J. Nucl. Phys. **29** (1979) 421.
- [32] N. Tanaka, Y. Suzuki, K. Varga and R. G. Lovas, Phys. Rev. C **59** (1999) 1391.
- [33] J. Usukura and Y. Suzuki, Phys. Rev. A **66** (2002) 010502(R).
Y. Suzuki and J. Usukura, Nucl. Inst. Meth. B **221** (2004) 195.
- [34] E. Shuryak and I. Zahed, Phys. Lett. B **589** (2004) 21.
- [35] N. I. Kochelev, H.-J. Lee and V. Vento, Phys. Lett. B **594** (2004) 87.
- [36] A. M. Lane and R. G. Thomas, Rev. Mod. Phys. **30** (1958) 257.
- [37] H. Horiuchi and Y. Suzuki, Prog. Theor. Phys. **49** (1973) 1974.

TABLE V: Decompositions of the Θ^+ resonances into the spin, isospin and color channels of the diquark model. See Tables II and III for the channel labels. $T_{1234} = 0$ and $\Gamma_{1234} = (10)$ are abbreviated. π is the parity of the channel wave function with respect to the diquark-diquark exchange. The AL1 potential is used.

$S_{12}T_{12}\Gamma_{12}$	$S_{34}T_{34}\Gamma_{34}$	S_{1234}	π	$P_c(\frac{1}{2}^-)$	$P_c(\frac{1}{2}^+)$
0 0 (01)	0 0 (01)	0	-1	0.0005	0.2067
0 0 (01)	1 0 (20)	1	-1	0.0017	0.0457
0 0 (01)	1 0 (20)	1	+1	0.4933	0.0272
0 1 (01)	1 1 (01)	1	-1	0.0008	0.0316
0 1 (01)	1 1 (01)	1	+1	0.0008	0.0316
0 1 (20)	1 1 (01)	1	-1	0.0012	0.0310
0 1 (20)	1 1 (01)	1	+1	0.1649	0.0126
1 1 (01)	1 1 (01)	0	-1	0.0003	0.0062
1 1 (01)	1 1 (01)	1	+1	0.3290	0.0215
0 0 (01)	0 0 (20)	0	-1	0.0002	0.0149
0 0 (01)	0 0 (20)	0	+1	0.0002	0.0149
0 0 (01)	1 0 (01)	1	-1	0.0007	0.0150
0 0 (01)	1 0 (01)	1	+1	0.0007	0.0150
0 1 (01)	1 1 (20)	1	-1	0.0000	0.0123
0 1 (01)	1 1 (20)	1	+1	0.0006	0.0068
0 1 (01)	0 1 (20)	0	-1	0.0001	0.0415
0 1 (01)	0 1 (20)	0	+1	0.0001	0.0415
1 1 (01)	1 1 (20)	0	-1	0.0003	0.1151
1 1 (01)	1 1 (20)	0	+1	0.0003	0.1151
1 0 (01)	1 0 (20)	0	-1	0.0001	0.0415
1 0 (01)	1 0 (20)	0	+1	0.0001	0.0415
1 1 (01)	1 1 (20)	1	-1	0.0008	0.0166
1 1 (01)	1 1 (20)	1	+1	0.0008	0.0166
1 0 (01)	1 0 (20)	1	-1	0.0006	0.0299
1 0 (01)	1 0 (20)	1	+1	0.0006	0.0299
0 1 (01)	0 1 (01)	0	-1	0.0000	0.0000
0 0 (20)	1 0 (01)	1	-1	0.0000	0.0041
0 0 (20)	1 0 (01)	1	+1	0.0005	0.0080
1 0 (01)	1 0 (01)	0	-1	0.0000	0.0000
1 0 (01)	1 0 (01)	1	+1	0.0006	0.0057
				1.0000	1.0000

TABLE VI: Decompositions of the Θ^+ resonances into the spin, isospin and color channels of the baryon-meson model. See Tables II and III for the channel labels. The AL1 potential is used.

$S_{12}T_{12}\Gamma_{12}$	$S_{123}T_{123}\Gamma_{123}$	$S_{45}T_{45}\Gamma_{45}$	$P_c(\frac{1}{2}^-)$	$P_c(\frac{1}{2}^+)$
0 0 (01)	$\frac{1}{2} \frac{1}{2}$ (00)	0 $\frac{1}{2}$ (00)	0.0022	0.0588
0 0 (01)	$\frac{1}{2} \frac{1}{2}$ (00)	1 $\frac{1}{2}$ (00)	0.0011	0.1615
1 1 (01)	$\frac{1}{2} \frac{1}{2}$ (00)	0 $\frac{1}{2}$ (00)	0.1529	0.0179
1 1 (01)	$\frac{1}{2} \frac{1}{2}$ (00)	1 $\frac{1}{2}$ (00)	0.0512	0.0124
0 1 (01)	$\frac{1}{2} \frac{1}{2}$ (00)	0 $\frac{1}{2}$ (00)	0.0006	0.0222
0 1 (01)	$\frac{1}{2} \frac{1}{2}$ (00)	1 $\frac{1}{2}$ (00)	0.0002	0.0095
1 0 (01)	$\frac{1}{2} \frac{1}{2}$ (00)	0 $\frac{1}{2}$ (00)	0.0005	0.0066
1 0 (01)	$\frac{1}{2} \frac{1}{2}$ (00)	1 $\frac{1}{2}$ (00)	0.0002	0.0028
0 0 (01)	$\frac{1}{2} \frac{1}{2}$ (11)	0 $\frac{1}{2}$ (11)	0.1841	0.0352
0 1 (20)	$\frac{1}{2} \frac{1}{2}$ (11)	0 $\frac{1}{2}$ (11)	0.0623	0.0267
1 0 (20)	$\frac{1}{2} \frac{1}{2}$ (11)	0 $\frac{1}{2}$ (11)	0.0622	0.0266
1 1 (01)	$\frac{1}{2} \frac{1}{2}$ (11)	0 $\frac{1}{2}$ (11)	0.0330	0.0642
0 0 (01)	$\frac{1}{2} \frac{1}{2}$ (11)	1 $\frac{1}{2}$ (11)	0.0615	0.0175
0 1 (20)	$\frac{1}{2} \frac{1}{2}$ (11)	1 $\frac{1}{2}$ (11)	0.0209	0.0365
1 0 (20)	$\frac{1}{2} \frac{1}{2}$ (11)	1 $\frac{1}{2}$ (11)	0.0209	0.0470
1 1 (01)	$\frac{1}{2} \frac{1}{2}$ (11)	1 $\frac{1}{2}$ (11)	0.0113	0.0701
0 0 (20)	$\frac{1}{2} \frac{1}{2}$ (11)	0 $\frac{1}{2}$ (11)	0.0002	0.0082
0 1 (01)	$\frac{1}{2} \frac{1}{2}$ (11)	0 $\frac{1}{2}$ (11)	0.0002	0.0190
1 0 (01)	$\frac{1}{2} \frac{1}{2}$ (11)	0 $\frac{1}{2}$ (11)	0.0004	0.0347
1 1 (20)	$\frac{1}{2} \frac{1}{2}$ (11)	0 $\frac{1}{2}$ (11)	0.0006	0.0201
0 0 (20)	$\frac{1}{2} \frac{1}{2}$ (11)	1 $\frac{1}{2}$ (11)	0.0002	0.0127
0 1 (01)	$\frac{1}{2} \frac{1}{2}$ (11)	1 $\frac{1}{2}$ (11)	0.0002	0.0319
1 0 (01)	$\frac{1}{2} \frac{1}{2}$ (11)	1 $\frac{1}{2}$ (11)	0.0002	0.0281
1 1 (20)	$\frac{1}{2} \frac{1}{2}$ (11)	1 $\frac{1}{2}$ (11)	0.0004	0.1092
1 1 (01)	$\frac{3}{2} \frac{3}{2}$ (00)	1 $\frac{1}{2}$ (00)	0.1239	0.0299
1 0 (20)	$\frac{3}{2} \frac{3}{2}$ (11)	1 $\frac{1}{2}$ (11)	0.1652	0.0343
1 1 (01)	$\frac{3}{2} \frac{3}{2}$ (11)	1 $\frac{1}{2}$ (11)	0.0419	0.0185
1 0 (01)	$\frac{3}{2} \frac{3}{2}$ (00)	1 $\frac{1}{2}$ (00)	0.0006	0.0118
1 0 (01)	$\frac{3}{2} \frac{3}{2}$ (11)	1 $\frac{1}{2}$ (11)	0.0004	0.0141
1 1 (20)	$\frac{3}{2} \frac{3}{2}$ (11)	1 $\frac{1}{2}$ (11)	0.0004	0.0119
			1.0000	1.0000